Nuclear magnetic resonance study of fluorine-graphite intercalation compounds

Nuclear magnetic resonance study of fluorine–graphite intercalation compounds

A M Panich†‖, T Nakajima‡, H-M Vieth§, A F Privalov§ and S D Goren†

† Department of Physics, Ben-Gurion University of the Negev, PO Box 653, Be'er Sheva 84105, Israel
‡ Division of Polymer Chemistry, Graduate School of Engineering, Kyoto University, Kyoto 606, Japan
§ Institute of Experimental Physics, Free University, Arnimallee 14, D-14195 Berlin, Germany

Abstract. To study the origin of semimetal–metal and metal–insulator transformations, localization effects and C–F bonding in fluorine-intercalated graphite $C_x F$, ^{13}C and ^{19}F NMR investigations have been carried out for a wide range of fluorine content, $3.8 \leqslant x \leqslant 12.7$. Fluorine spectra for small fluorine content, $x > 8$, are attributed to mobile fluorine acceptor species which are responsible for the increase of electric conductivity in the dilute compound. When increasing the fluorine content to $x \sim 8$ corresponding to the maximum electric conductivity, covalent C–F bonds start to occur. The number of these bonds grows with fluorine content resulting in a decrease in conductivity which is caused by a percolation mechanism rather than by a change in bond length. A difference in ^{19}F chemical shift for fluorine-intercalated graphite $C_x F$ and covalent graphite fluoride $(CF)_n$ has been observed and is attributed to different C–F bonding in these compounds.

1. Introduction

Fluorine-intercalated graphite and graphite fluorides have attracted much attention because of their potential for industrial application as lubricants and as cathode materials in lithium batteries [1, 2]. They are now considered a unique family of graphite intercalation compounds (GICs) which exhibits a behaviour that is strikingly different from all other known GICs [3–11]. For most GICs the in-plane electrical conductivity σ initially increases upon intercalation due to the increase in charge carrier density resulting from injection of carriers (electrons for donors and holes for acceptors) from the intercalate species to the graphite layers, often resulting in an increase in conductivity by an order of magnitude and transformation of the semimetallic graphite into a metal. Upon further intercalation, the conductivity decreases, but only slightly. In fluorine-intercalated graphite, $C_x F$, the in-plane conductivity also increases with the increase of fluorine concentration for dilute compounds, $x > 8$, has a plateau for $8 > x > 6$, but then, in contrast to the other GICs, decreases sharply with further intercalation [3, 4, 6, 11]. The temperature dependence of the resistance suggests that $C_x F$ undergoes a transition from a system of weakly localized carriers ($x > 3.6$) to a system of strongly localized carriers ($x < 3.6$) [6].

Based on XPS and x-ray data, it was suggested that the planarity of carbon sheets in $C_x F$ is maintained and the nature of C–F bonding changes from ionic to a more covalent character

‖ Corresponding author. E-mail address: pan@bgumail.bgu.ac.il.

(called semicovalent or semi-ionic) with increased fluorine content [5, 7, 10–12]. Such an increase in the covalent character of the C–F bond was expected to reduce the carrier density and cause a rapid decrease in conductivity. However, a percolation mechanism due to the increasing number of covalent C–F bonds may also play an important role [3, 4, 13]. For the dilute, purely ionic compound, F$^-$ is considered an acceptor which transforms semimetallic graphite into a metal [5, 7, 10–12].

The objective of the present paper is the NMR investigation of F-GICs to study C–F bonding and to explain the semimetal–metal and metal–insulator transformations and the localization effects in fluorine-intercalated graphite. Chemical shifts measured by NMR are sensitive to local bonding and site distribution effects, and line shape analysis yields information on atomic mobility. ^{13}C and ^{19}F NMR study of C$_x$F compounds in a wide range of fluorine content, $3.8 \leqslant x \leqslant 12.7$, has been performed. These fluorine concentrations cover both a regime of increase in conductivity as well as an intermediate region in which the conductivity has a plateau and starts to decrease. For comparison, graphite fluorides (CF)$_n$ and (C$_2$F)$_n$, have also been studied. These compounds are insulators, C–F bonds are completely covalent and the carbon skeletons are no longer planar but consist of carbon layers corrugated due to sp^3 hybridization and with covalent C–F bonds lined up from both sides perpendicular to this plane [14–18].

2. Experimental details

Samples of C$_x$F with $x = 3.8$, 4.6, 6.0 and 6.5 have been prepared by fluorination of graphite fibres heat treated at 2850–2900 °C. Graphite fibres were placed in a pre-evacuated (by a rotary pump) reactor and were allowed to react with fluorine gas (1 atm) for 14 to 60 days at room temperature in the presence of traces of HF as catalyst [12]. The other samples with $x = 4.5$, 6.9, 7.3, 8.0, 9.1, 9.6, 10.2 and 12.7 have been prepared by fluorination of powdered natural graphite (57–74 μm) at the same conditions. All samples were sealed into quartz tubes in a dry nitrogen atmosphere. X-ray data on interlayer distances and stage numbers are given in table 1. Graphite fluorides (CF)$_n$ and (C$_2$F)$_n$ have been prepared by graphite fluorination at temperatures 450–500 and 350–400 °C, respectively.

Table 1. Interlayer distances and stage numbers of fluorine-intercalated graphite.

Compound	Stage	I_c (A)
C$_{3.8}$F	1	5.15
C$_{4.6}$F	1	5.08
	2	9.24
C$_{6.0}$F	2	9.25
C$_{6.0}$F	2	9.29
C$_{6.5}$F	2	9.64
C$_{4.5}$F	1	4.69, 5.24
	2	9.41
C$_{6.9}$F	2	9.55
	3	12.74
C$_{7.3}$F	2	9.57
	3	12.76
C$_{8.0}$F	3	12.87
C$_{9.1}$F	3	12.76
C$_{9.6}$F	3	12.77
C$_{9.6}$F	4	16.32
C$_{10.2}$F	4	16.38
C$_{12.7}$F	4	16.90

Room temperature ^{19}F NMR spectra have been recorded at 282.4 MHz ($B_0 = 7.05$ T) with a CXP Bruker pulse NMR spectrometer using Fourier transformation of the free induction decays. Chemical shifts have been measured relative to freon, $CFCl_3$. Since the room temperature ^{19}F spectra consist of broad and narrow lines which exhibit different spin–spin relaxation times T_2 (e.g., $T_{2br} = 92$ μs and $T_{2nar} = 2.7$ ms respectively for $C_{4.5}F$), we also recorded the narrow line only using an echo sequence with a delay between pulses longer than T_{2br} making the broad line disappear. By subtraction of the narrow line from the total spectrum we obtained the broad line separately. In addition, temperature variable ^{19}F NMR spectra between 77 and 300 K have been recorded at 28.05 MHz ($B_0 = 0.7$ T) with a Tecmag pulse NMR spectrometer using Fourier transformation of the phase cycled solid echo. ^{13}C NMR spectra at room temperature have been recorded at 75.48 MHz with a CXP Bruker pulse NMR spectrometer using Fourier transformation of the phase cycled Hahn echo. [13]C chemical shifts are given relative to TMS. To check the residual hydrogen, ^{1}H NMR at 28.05 MHz has also been performed.

3. Results and discussion

[13]C spectra of C_xF at room temperature are given in figure 1. All spectra are similar showing a shape which is characteristic for an axially symmetric chemical shielding tensor, although the shoulder at $\delta_\parallel$ is not very pronounced. Because there is no large contribution of the carbon–fluorine dipolar coupling present in these spectra, they were attributed to
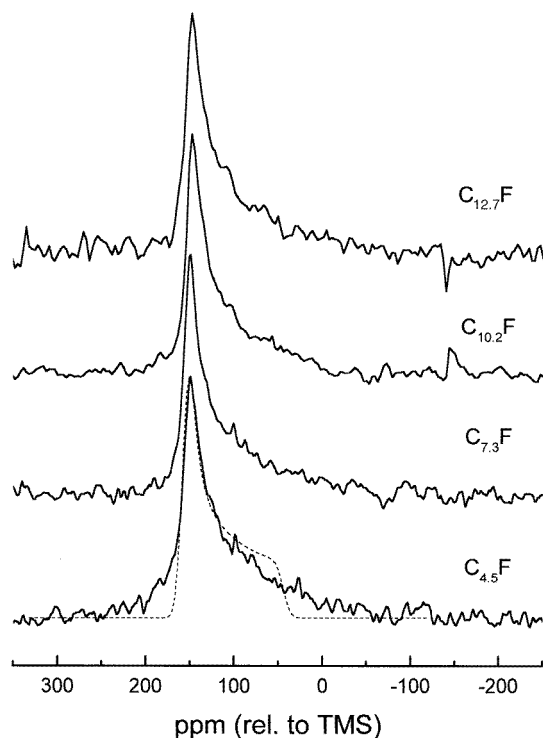

Figure 1. ^{13}C NMR spectra of fluorine-intercalated graphite at room temperature. The simulated spectrum for axially symmetric chemical shielding tensor is shown by dashed line.

carbons that are not bound to fluorine. The positions of the centre of gravity δ_i and of the singularity at $\delta_\perp$ for all spectra practically coincide. From the line shape analysis, δ_i and the chemical shielding anisotropy $\delta_a = \delta_\parallel - \delta_\perp$ are found to be $\delta_i = 112 \pm 5$ ppm and $\delta_a = -120 \pm 10$ ppm relative to TMS. The obtained value of δ_i is close to the ^{13}C chemical shift determined in graphite ($\delta_i = 119$ ppm) and in GICs of acceptor type, GICA ($\delta_i = 113$ to 130 ppm) [19, 20]. The value of chemical shielding anisotropy δ_a is in satisfactory agreement with experimental data for GICs of acceptor type which show δ_a from -120 to -150 ppm [19–21] and with the value of δ_a for GICA calculated from the band structure ($\delta_a \sim -140$ ppm), which is shown to be practically independent of charge transfer and the intercalate concentration [20]. We notice that for GICAs, Knight shift is negligible and the shifts come mainly from a paramagnetic (Ramsey) term which arises from the mixing between the occupied ground state and the unoccupied excited states due to the partial unquenching of the orbital moment of the electrons in the external magnetic field.

Low field ($B_0 = 0.7$ T) ^{19}F measurements show that, for most of the samples (except for dilute compounds, $x > 8$), the ^{19}F spectra at room temperature consist of two lines (figure 2): a narrow line ($\Delta \nu \sim 1$ kHz) from mobile fluorine species and a broad line ($\Delta \nu$ between ~ 11 and ~ 18 kHz for $x = 8$ and 3.8, respectively) from the 'rigid lattice'. The broad line is typical for graphite fluorides with covalent C–F bonds [16, 18, 22]; its width is mostly due to dipolar coupling among the fluorines. At high magnetic field, 7 T, the room temperature spectra also consist of broad and narrow lines, except for the dilute samples, $x > 8$, which practically show only a narrow line (figure 3). When going from 0.7 to 7 T, the width of the narrow line increases by a factor of ten, showing that shielding anisotropy determines the line width. The line shape is characteristic for an axially symmetric shielding tensor with $\delta_\parallel - \delta_\perp = 46$ ppm which results from motional averaging (figure 3). Broadening
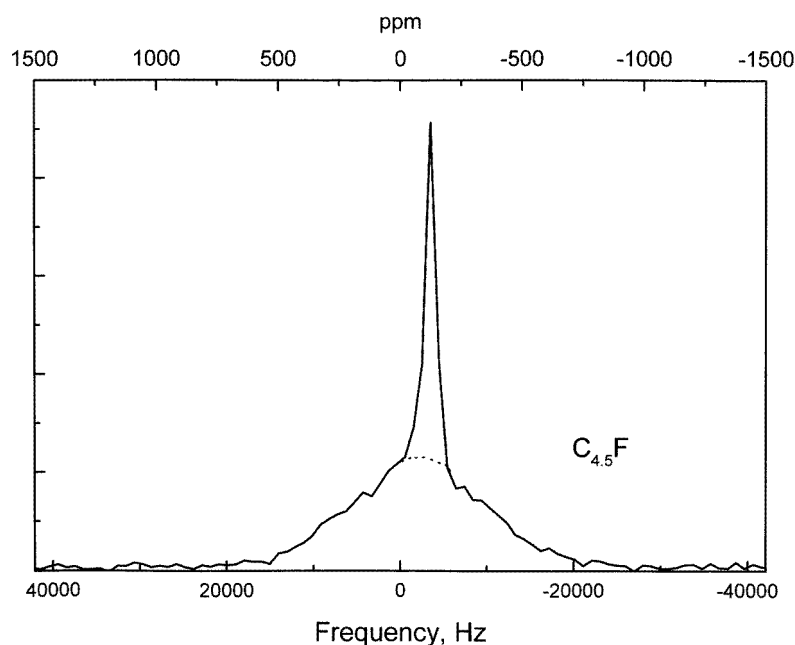

Figure 2. Room temperature ^{19}F NMR spectrum of fluorine-intercalated graphite $C_{4.5}F$ at 28.07 MHz.
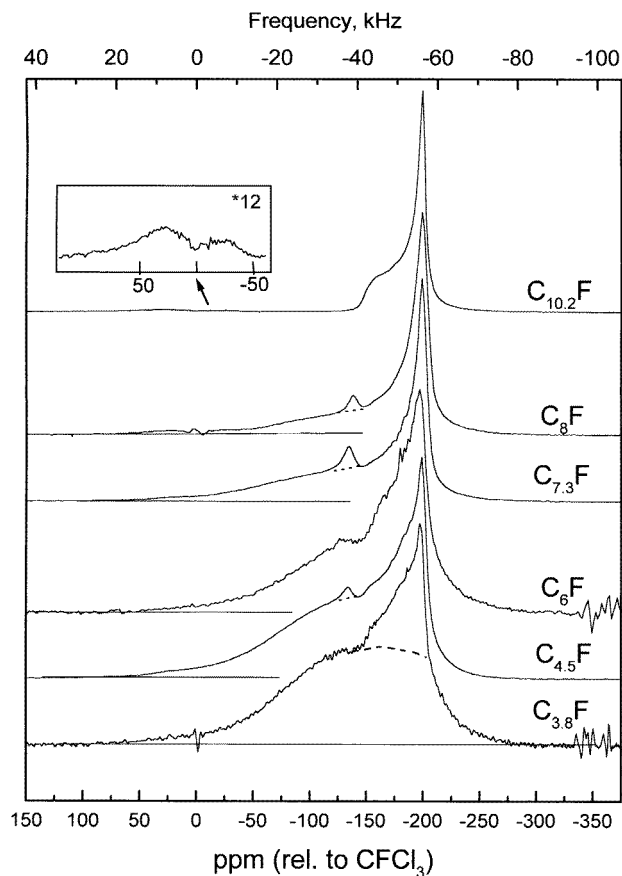
Figure 3. Room temperature ^{19}F NMR spectra of fluorine-intercalated graphite at 282.4 MHz. In addition to an intensive broad line in the range between -30 and -270 ppm, weak broad peaks around $\delta \sim 0$ ppm (shown in inset) exist; for more fluorinated compounds the fine structure is not pronounced.

of this line at the temperature range 150 to 115 K indicates freezing of the mobility. The intensive broad line in the range between -30 and -270 ppm is asymmetric with its centre of gravity at $\delta \sim -150$ ppm. It is attributed to 'rigid' covalent (or semicovalent) C–F bonds in the graphite galleries. When going from 0.7 to 7 T, its width increases only by a factor of ~ 2. Thus the contributions to the line shape from the chemical shift anisotropy and from [19]F–[19]F dipole–dipole interactions are of the same order. Since the shape of this line is not typical for the convolution of an axially or nonaxially symmetric chemical shielding tensor with a dipolar broadened line, we attribute it to a distribution of chemical shifts for different F sites, i.e. it is expected that interior CF groups adjacent to aromatic sp^2 carbon and to sp^3 CF species show different chemical shift. This is in agreement with transmission electron microscopy (TEM) measurements which have established the presence of disorder in fluorine-intercalated graphite, buckling of the stiff graphene planes and formation of islands of various fluorine concentrations [9]. The signal intensity in the range between -50 and -120 ppm may be partially due to a contribution of CF_2 and CF_3 groups resulting from the fluorination of edges of the carbon planes. In addition to an intensive broad line

mentioned above, there are also weak broad peaks around $\delta \sim 0$ ppm; for compounds with higher fluorination the fine structure of these peaks is not pronounced (figure 3). Based on the ^{19}F chemical shift, this low field tail may be attributed to –COF and –COF$_2$ groups [23, 24].

One can notice that in the region from $x = 8$ to 3.8, in which the conductivity has a plateau and starts to decrease with increasing fluorine content, the position and shape of the broad line are practically independent of fluorine content (figure 3). This is better seen from the spectra of the broad line only (figure 4), where the narrow line and the impurity spike at -130 ppm were subtracted with the procedure described in section 2. The obtained result indicates that the character of C–F bonds in the region from $x = 8$ to 3.8 is almost unchanged. These data are in agreement with XPS measurements [12] showing that the binding energy of the fluorine 1s (F_{1s}) electron is unchanged in the range of $4 < x < 9$. The intensity ratio of broad to narrow line decreases with decrease of fluorine content (figure 5), until the broad line practically disappears at $x \sim 9$. Moreover as mentioned above, the increase in conductivity stops just at the fluorine content corresponding to $x \sim 8$, when, from our NMR data, covalent C–F bonds occur. The correlation between the growth in the number of the covalent C–F bonds and the drop in conductivity for the fluorine concentrations above the value corresponding to σ_{max} allows us to suggest that this drop is caused by a percolation mechanism rather than by a change in bond length. When such a covalent C–F bond is formed, each fluorine atom blocks one node in the conductive graphite network, and this node does not take part in the conductivity any longer. The critical number of unblocked nodes (threshold for percolation) for a two-dimensional honeycomb lattice is 70% [25]. Conductivity measurements of C$_x$F show that the conductivity drops to zero at $x \sim 3$, which is just around 70%. The intensity ratio of the broad to narrow line for $x = 3$ estimated from our spectra shows the number of unbound carbons around 73%, in
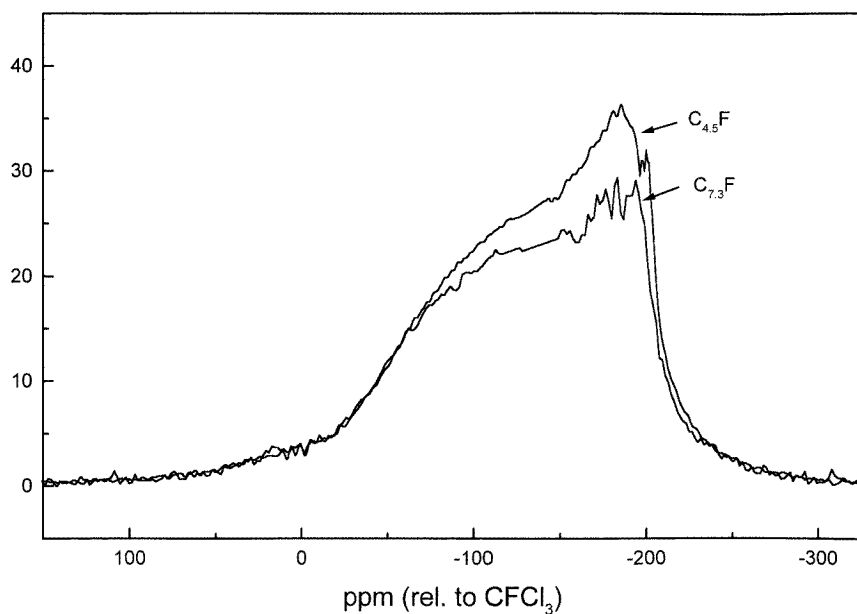

Figure 4. Broad ^{19}F line of fluorine-intercalated graphite at room temperature and $\nu_0 = 282.4$ MHz.
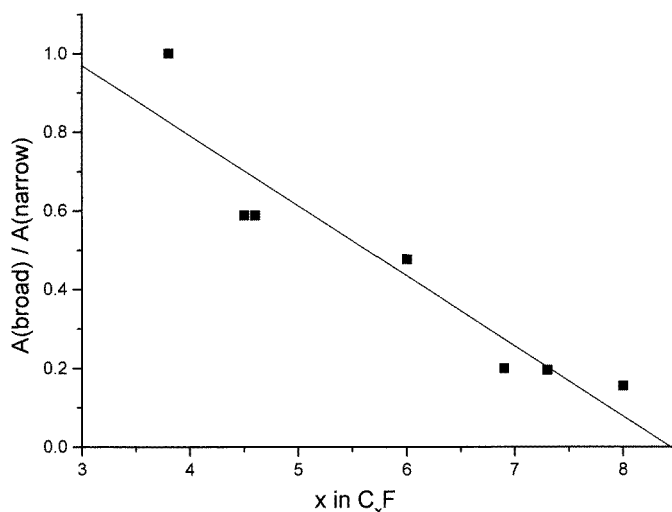
Figure 5. The amplitude ratio of broad to narrow ^{19}F line in fluorine-intercalated graphite at room temperature ($\nu_0 = 282.4$ MHz).

satisfactory agreement with the aforementioned theoretical value. Thus the covalent C–F bonds may be considered to be responsible for the percolation decrease in conductivity.

Concerning the nature of the C–F chemical bond, it is nevertheless different for fluorine–graphite intercalation compound and graphite fluorides. The fully fluorinated compound $(CF)_n$, which is an insulator and exhibits completely covalent C–F bonds [12], shows a chemical shift different from C_xF, indicating the difference in chemical bond (figure 6). This picture is consistent with XPS measurements [12] of the binding energy of an F_{1s} electron. As was shown, the energy stays unchanged in the range of $4 < x < 9$ and becomes different for $x < 4$. The $(CF)_n$ line shows a shift to high field in comparison to C_xF. This is in contradiction with the common fluorine chemical shift scale where a more covalent compound exhibits a down-field shift [26, 27]. Thus this difference in chemical shift can hardly be described in terms of ionicity and covalency. From our data, we have to conclude that CF groups adjacent to carbons in nonsaturated C_xF compound exhibit a down-field chemical shift, while those adjacent to sp^3-hybridized CF species in the fully fluorinated and saturated compound $(CF)_n$ exhibit high-field chemical shifts. It is noteworthy that the chemical shifts for fluorine nuclei in aliphatic, olefinic, aromatic and ionic compounds overlap extensively [26]†

Let us now discuss the increase in conductivity with increasing fluorine content for the dilute compounds $x > 8$. In this regime, the room temperature spectra are represented by only the narrow line attributed to mobile fluorines. One can suggest that this species is an electron acceptor which, as for the other GICs, injects holes into the host graphite layers and thus is responsible for the increase of conductivity for dilute compounds. This increase comes to an end at $x \sim 8$ when the covalent C–F bonds start to block the nodes of the

---

† We notice that our data on chemical shift of $(CF)_n$ prepared from natural graphite flake and petroleum coke, $\delta = -174\pm10$ and -162 ± 10 ppm respectively, are in satisfactory agreement with the data of Hamwi who obtained $\delta(CF)_n = -197\pm20$ ppm [28] but they contradict the measurements of Wilkie who determined $\delta(CF)_n = -55$ ppm [29]. $(C_2F)_n$ shows $\delta = -165\pm10$ ppm in agreement with $\delta = -145\pm15$ ppm measured for $(C_2F)_n$ intercalated with BrF_3, ClF_3, acetone and the other molecules [18].
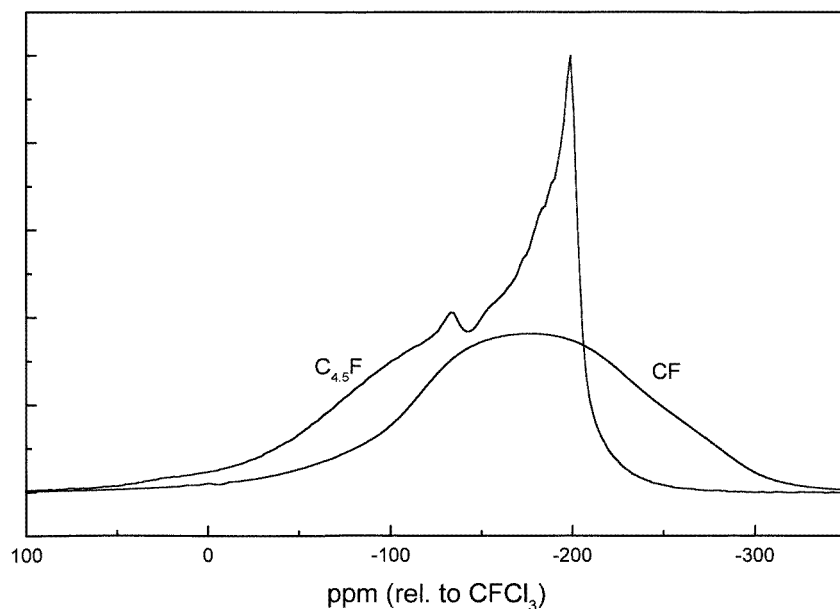
Figure 6. Room temperature ^{19}F NMR spectra of fluorine-intercalated graphite $C_{4.5}F$ and graphite fluoride $(CF)_n$ at 282.4 MHz.

conductive network. According to the XPS data, fluorine intercalated into graphite is of a purely ionic character at low concentrations and such F^- is an acceptor which transforms semimetallic graphite into a metal [5, 7, 10–12]. It should be noticed that no examples of such a purely ionic C–F bond have been observed for fluorine–carbon compounds other than F-GICs. Such a bond is supposed to be weak and to cause fluorine mobility just as observed in our experiment. The value of the ^{19}F chemical shift of the narrow line $\delta = -185 \pm 5$ ppm is close to the shift of a fluorine ion in ionic crystals such as NaF and MgF_2, -221 and -187 ppm, respectively [30, 31]. The signal is typical for diffusing ions and molecules whose shape is governed by anisotropic electron–nuclear interactions partially averaged by diffusion [32–34]. Thus the attribution of the narrow line to mobile fluorine ions seems realistic. One can notice that the shift of the narrow line is also close to the shift of the HF molecule (-192 ppm [26, 27]); moreover, a narrow ^{1}H NMR signal at room temperature is also observed in our compounds suggesting that HF species are present. However, since the principal axes of dipole–dipole and chemical shift tensors in the HF molecule coincide, the motional averaging is the same for both tensors; thus doublet structure caused by ^{1}H–^{19}F dipolar coupling must appear when chemical shielding anisotropy is not completely averaged. The absence of such a doublet structure does not allow us to assign the narrow signal to HF molecules. It is noteworthy that narrow ^{19}F lines with the same temperature behaviour were obtained by Touhara *et al* for both the fluorine-intercalated graphite $C_{6.4}F$ and the stage-2 C_xHF_2 compound [35].

Measurements of the temperature dependence of resistivity and expansion coefficient show an anomaly around 150 K which was attributed to a phase transition [5, 11, 35–37]. As mentioned above, our spectra show the freezing of mobility at 150–115 K. Such a correlation is interesting and allows us to suggest a correlation between these two effects; however, the study of such a correlation is beyond the scope of our paper.

4. Summary

^{13}C and ^{19}F NMR investigation of fluorine-intercalated graphite C_xF has been carried out for a wide range of fluorine content, $3.8 \leqslant x \leqslant 12.7$. The ^{19}F line shape shows a distribution of chemical shifts for different F sites. Differences in ^{19}F chemical shift for fluorine-intercalated graphite C_xF and covalent graphite fluorides $(CF)_n$ have been obtained and are attributed to different C–F bonding in these compounds. Fluorine spectra for $x > 8$ are attributed to a mobile fluorine acceptor species which is responsible for the increase in conductivity with increasing fluorine content in the dilute compound. At a fluorine content of $x \sim 8$ corresponding to the maximum of conductivity, the formation of the covalent C–F bonds starts. The number of such bonds increases with growing fluorine content resulting in a drop in conductivity which we attribute to a percolation mechanism rather than to the change in bond length. These results provide an atomic level rationale for understanding of physical properties of fluorine–graphite intercalation compounds.

Acknowledgment

References

[1] Tsuya Y 1995 *Fluorine–Carbon and Fluoride–Carbon Materials* ed T Nakajima (New York: Dekker) p 355
[2] Yazami R 1995 *Fluorine–Carbon and Fluoride–Carbon Materials* ed T Nakajima (New York: Dekker) p 251
[3] Vaknin D, Palchan I, Davidov D, Selig H and Moses D 1986 *Synth. Met.* **16** 349
[4] Ohana I, Palchan I, Yakobi Y, Davidov D and Selig H 1988 *Phys. Rev.* B **38** 12 627
[5] Piraux L, Bayot V, Issi J P, Dresselhaus M S, Endo M and Nakajima T 1990 *Phys. Rev.* B **41** 4961
[6] di Vittorio S L, Dresselhaus M S, Endo M and Nakajima T 1991 *Phys. Rev.* B **43** 1313
[7] di Vittorio S L, Dresselhaus M S, Endo M and Nakajima T 1991 *Phys. Rev.* B **43** 12 304
[8] Rao A M, Fung A W P, di Vittorio S L, Dresselhaus M S, Dresselhaus G, Endo M, Oshida K and Nakajima T 1992 *Phys. Rev.* B **45** 6883
[9] Oshida K, Endo M, Nakajima T, di Vittorio S L, Dresselhaus M S and Dresselhaus G 1993 *J. Mater. Res.* **8** 512
[10] di Vittorio S L, Dresselhaus M S and Dresselhaus G 1993 *J. Mater. Res.* **8** 1578
[11] Dresselhaus M S, Endo M and Issi J-P 1995 *Fluorine–Carbon and Fluoride–Carbon Materials* ed T Nakajima (New York: Dekker) p 95
[12] Nakajima T 1995 *Fluorine–Carbon and Fluoride–Carbon Materials* ed T Nakajima (New York: Dekker) p 1
[13] Panich A M, Nakajima T and Goren S D 1997 *Chem. Phys. Lett.* **271** 381
[14] Kita Y, Watanabe N and Fujii Y 1979 *J. Am. Chem. Soc.* **101** 3832
[15] Mahajan V K, Badachape R B and Margrave J L 1974 *Inorg. Nucl. Chem. Lett.* **10** 1003
[16] Panich A M, Danilenko A M and Gabuda S P 1985 *Dokl. Akad. Nauk SSSR* **281** 389
[17] Yudanov N F and Chernyavsky L I 1987 *J. Struct. Chem.* **28** 534
[18] Panich A M 1993 *Colloids Surf.* **72** 19
[19] Resing H A, Milliken J, Dominques D D and Iton L E 1985 *Proc. 17th Bienn. Conf. on Carbon* (Lexington, KY: Kentucky University Press)
[20] Tsang T and Resing H A 1985 *Solid State Commun.* **53** 39
[21] Conard J, Gutierrez-Le Brun M, Laugine P and Estrade-Szwarckopf H 1980 *Synth. Met.* **2** 227
[22] Panich A M 1985 *J. Struct. Chem.* **26** 888
[23] Zschunke A 1971 *Kernmagnetische Resonanzspectroskopie in der Organischen Chemie* (Berlin: Akademie)
[24] Wray V 1983 *Annual Reports on NMR Spectroscopy* vol 14, ed G A Webb (London: Academic)
[25] Shklovskii B and Efros A 1984 *Electronic Properties of Doped Semiconductors* (Berlin: Springer)
[26] Gunther H 1980 *NMR Spectroscopy* (New York: Wiley)
[27] Gabuda S P, Gagarinsky Yu V and Politschuk S A 1978 *NMR in Inorganic Fluorides* (Moscow: Atomizdat)
[28] Hamwi A, Daoud M, Djurado D, Cousseins J C, Fawal Z and Dupuis J 1991 *Synth. Met.* **44** 75

[29] Wilkie C A, Lin G-Yu and Haworth D T 1979 *J. Solid State Chem.* **30** 197
[30] Sears R E J 1974 *J. Chem. Phys.* **61** 4368
[31] Mehring M, Pines A, Rhim W-K and Waugh J S 1971 *J. Chem. Phys.* **54** 3239
[32] Panich A M, Belitskii I A, Moroz N K, Gabuda S P, Drebushchak V A and Seretkin Yu V 1990 *J. Struct. Chem.* **31** 56
[33] Panich A M 1996 *Appl. Spectrosc.* **50** 1452
[34] Panich A M 1994 *J. Magn. Reson.* A **111** 37
[35] Touhara H, Goto Y, Watanabe N, Imaeda K, Enoki T, Inokuchi H and Mizutani Y 1988 *Synth. Met.* **23** 461
[36] Nakajima T, Chang B, Fujiwara T, Watanabe N and Endo E 1988 *Carbon* **26** 213
[37] Tressaud A, Dordor P, Marquestaut E, Hagenmuller P, Fujimoto H and Flandrois S 1991 *Synth. Met.* **40** 179